THE JOURNAL OF PHYSICAL CHEMISTRY B

Article

pubs.acs.org/JPCB

Supramolecular Control of Photochemical and Electrochemical Properties of Two Oligothiophene Derivatives at the Air/Water Interface

Sophiya Selector,[†] Olga Fedorova,*[,‡,§] Elena Lukovskaya,[‡] Alexander Anisimov,[‡] Yuri Fedorov,[§] Nina Tarasova,[†] Oleg Raitman,[†] Frederic Fages,[∥] and Vladimir Arslanov[†]

[†]A.N. Frumkin Institute of Physical Chemistry and Electrochemistry of Russian Academy of Sciences, Leninsky prosp. 31-4, Moscow, 119991,GSP-1, Russia

[‡]Chemistry Department of Moscow State University, 1-3 Leninskiye Gory, Moscow, 119991, GSP-1, Russia

[§]A.N. Nesmeyanov Institute of Organoelement Compounds of Russian Academy of Sciences, Vavilova str., 28, Moscow, 119991,GSP-1, Russia

[∥]CINaM UPR 3118 CNRS - Universite de la Méditerranée, Campus de Luminy, Case 913, Marseille, 13288 France

ABSTRACT: Two geometric isomers of oligothiophene derivatives containing two crowned styryl fragments in 2- or 3-positions of thiophene rings are able to form stable monolayers on the water subphase. The organizing of crown-containing oligothiophenes in monolayers is guided by the π-stacking interaction of hydrophobic styrylthiophene fragments and interaction of hydrophilic macrocycles with the water subphase. The difference in structure of oligothiophene molecules leads to the formation of distinct monolayer architectures with various electrochemical and optical characteristics.

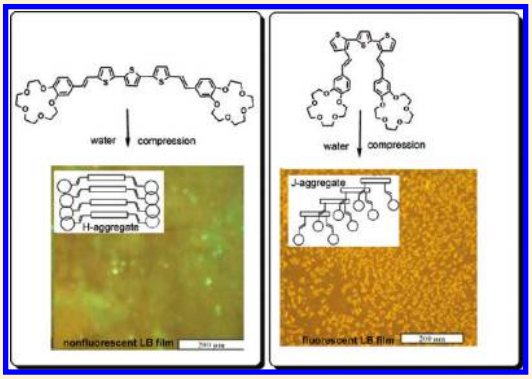

Over the last few decades, ultrathin films (Langmuir monolayers, Langmuir–Blodgett films, self-assembled monolayers, cast films) prepared from conjugated organic materials whether either polymers or oligomers have obtained considerable attention.[1−10] Investigations of the ultrathin film materials are motivated by the possible technological applications, such as organic light emitting diodes (OLEDs),[11−16] field effect transistors (FETs),[17−20] and photovoltaic cells.[21] Thin films based on conjugated materials are much favored for these kinds of applications since in general they can be easily prepared compared to the sophisticated processes of organic single crystal growth and can be tailored for special purposes in thickness and geometry in a well-defined way, e.g., multilayer preparation[22,23] or optical microcavities.[24,25]

Oligothiophenes[1−5,26−28] are one of the well-studied π-conjugated oligomeric model systems. This class of molecules has been a target for chemical tailoring in different groups worldwide[29,30] to provide a broad range of systems with well-defined chain lengths. Oligothiophene and its substituted derivatives have received particular attention, namely, since their electronic properties can be easily modulated upon substitution in the different positions along the conjugated backbone. Another way of modifying and enhancing the functional efficiency of oligothiophene building blocks is inclusion of various covalently attached functional groups within such molecules. In recent years, this approach has become paramount. One of these approach directions is to use conducting polymers bearing molecular recognizing groups in which highly selective host–guest interactions can modulate, switch, and amplify the electron transport properties.[31−34]

To obtain thin films of oligothiophene derivatives with high carrier mobility, it is crucially important that the organic molecules along with intramolecular charge mobility should be arranged in specific molecular architectures.[35] In particular, a high degree of molecular ordering and a special molecular orientation are required for efficient intermolecular charge migration and thus for best device performance. For example, it is well-known that twisting a conducting polymer's backbone from planarity can result in a conductivity drop as high as 10^5 or greater.[36]

In this research, we studied the architecture and properties of the monolayers and LB films[37] prepared from two isomeric oligothiophene derivatives (**I** and **II** in Scheme 1).

EXPERIMENTAL SECTION

Chemicals. The synthesis of **I** and **II** was described in refs 38 and 39.

Received: August 3, 2011
Revised: December 23, 2011
Published: January 3, 2012

Scheme 1

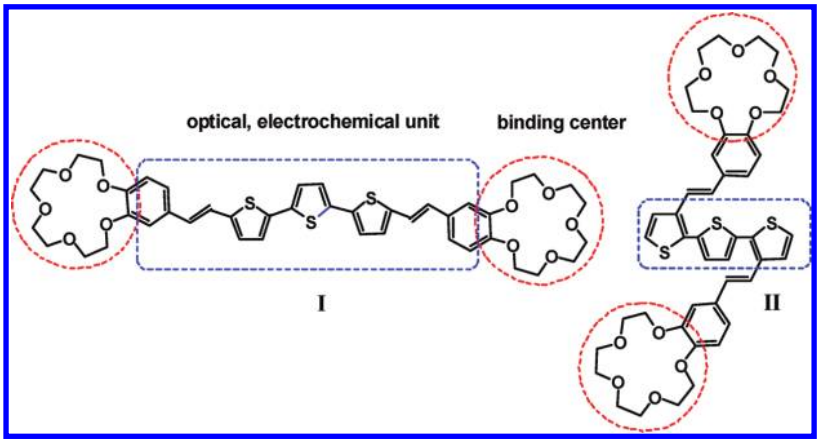

Langmuir Monolayers and Langmuir–Blodgett Films Investigation. The monolayers of crown-containing oligothiophenes **I** and **II** were formed from 10^{-4} M solutions in $CHCl_3$ (analytical grade). Deionized water 18 MΩ/cm, pH 5.6 (≪Vodolei≫, "Khimelektronika"), was used as a subphase. The monolayer compression isotherms were obtained using "KSV-2000" automated Langmuir trough. The surface pressure was measured by the Wilhelmy method using platinum plates. Solutions of crown-oligothiophenes were deposited on the subphase with a Gilson "Distriman" micropipet by 5 μL portions. The solvent evaporation time was ca. 15 min, and the speed of monolayer compression was 0.2 mm/s.

The monolayers were transferred onto solid substrates by the Langmuir–Blodgett technique under constant surface pressures of 20 or 30 mN/m. In dependence on the experimental method employed, quartz plates (UV–vis absorption spectroscopy and fluorescent measurements) and glass plates, covered with indium tin oxide (ITO) (electrochemistry and UV–vis absorption spectroscopy) or with gold layers as electrodes (electrochemistry and surface plasmon resonance spectroscopy), were used (the number of monolayers ranging from 1 to 4).

UV–visible spectra of LB films were measured in transmission mode on a CARY 5G spectrophotometer (Varian), at normal incidence and at room temperature, and also by a computerized SPECORD M40 spectrophotometer for the wavelength region of 200–900 nm.

Steady-state emission spectra of solutions and LB films were recorded in a right angle configuration with a Fluoromax-3 spectrofluorometer (Jobin Yvon). Excitation wavelength was adjusted each time to the maximum of the absorption band films.

Under the fluorescence microscopy experiments, the quartz plate covered with the monolayer was placed on the stage of a fixed-stage upright microscope (BX51WI from Olympus) equipped with a 100 W mercury lamp (U-LH100HG), a BX-RFA illuminator, and an U-MWBV2 (excitation at 400–440 nm, emission above 475 nm) or U-MNB2 (excitation at 470–490 nm, emission above 520 nm) filter cube. LMPF1 ×10, ×20, and ×50 objectives were used for imaging. Images were recorded with a DV465 Electron Multiplying CCD camera from Andor (Belfast, Northern Ireland). Acquisition times were on the whole in the 1–5 s range. At least three images were taken at different points of the monolayer. The lateral resolution of our setup is in the 0.4–0.6 μm range according to the numerical aperture of the objectives.

UV–visible differential reflection spectra of monolayers at the air/water interface (Langmuir monolayers) were obtained by a dual channel fiber optic spectrometer (Avantes, AvaSpec-2048-2) at normal incidence in accordance with the method described in refs 40 and 41.

Fluorescence spectra of monolayers at the air/water interface (Langmuir monolayers) were obtained by the same dual channel fiber optic spectrometer (Avantes, AvaSpec-2048-2) and LED light source; in this case, the angle of incidence was 45° relative to the water surface.

An electronic potentiostat "IPC-compact" and three-electrode electrochemical cell were used for electrochemical investigations of LB films. A standard Ag^+/AgCl electrode was employed as a reference. A platinum network cylindrical electrode was used as the counter electrode. The surface area of the counter electrode exceeded the area of working one by more than a factor of 100. The cyclic voltammetry (CV) measurements were carried out from +1.0 to −0.2 V against a Ag^+/AgCl reference electrode at a potential sweep of 0.1 V/s in water at 0.1 M $NaClO_4$.

Surface plasmon resonance (SPR) measurements were performed with a "Biosuplar 2" spectrophotometer (Analytical-μSystem, Germany) equipped with a laser diode with λ = 670 nm (0.2 mW power). The obtained data were processed with application of "Biosuplar 2" software (ver. 2.2.30). For SPR measurements, LB films of **I** and **II** were transferred onto SPR-plates (TF-1 glass, 20 × 20 mm, covered with 5 nm adhesive chromium layer and 50 nm polycrystalline gold layer, Analytical-μSystem).

RESULTS AND DISCUSSION

Synthesis and complex formation study of oligothiophenes **I** and **II** were described earlier.[38,39,42] According to the NMR spectroscopy data, both compounds are formed as *E*-isomers. The compounds **I** and **II** are differeny from each other in the position of styryl fragments. The oligothiophene **I** contains the substituents in the 2-position of thiophene rings, whereas, the styryl fragments in the molecule **II** are located in the position 3. The arrangement of two styryl fragments in the oligothiophene **II** molecule is opposite in direction (Scheme 1).[39] The structural variation between **I** and **II** should also cause the change in architectures (and properties) of the supramolecular assemblies formed on the air/water interface.

The molecules **I** and **II** consist of two styryl and tris(thiophene) hydrophobic parts and two hydrophilic crown

dx.doi.org/10.1021/jp2074122 | J. Phys. Chem. B 2012, 116, 1482–1490

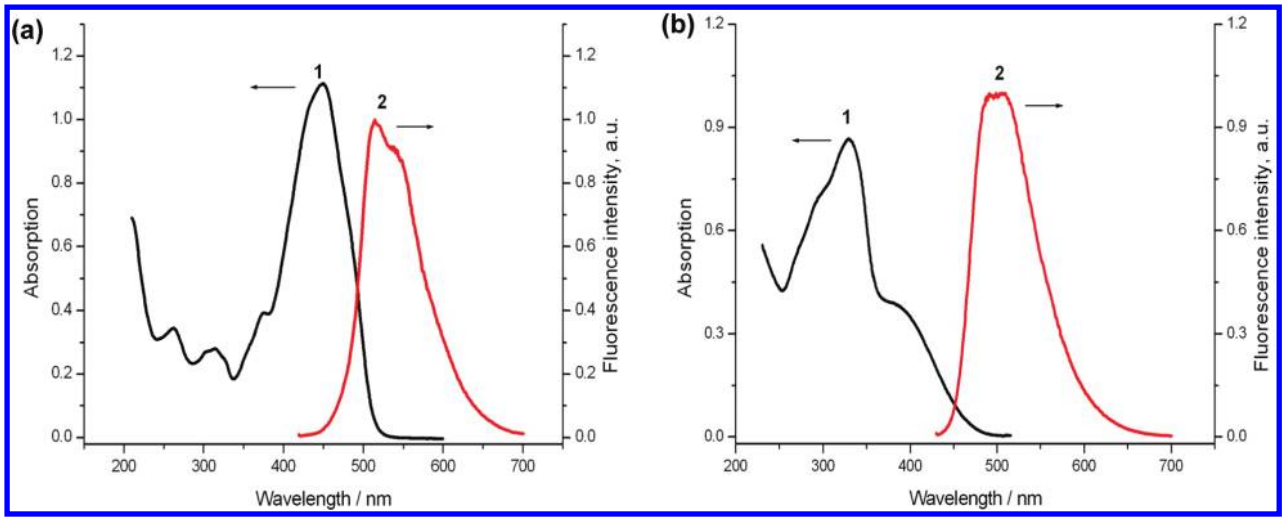

Figure 1. (a) Electronic absorption (1) and fluorescence emission (2) spectra of **I** ([**I**] = 2 × 10^{-5} M) in acetonitrile. (b) Electronic absorption (1) and fluorescence emission (2) spectra of **II** ([**II**] = 2 × 10^{-5} M) in acetonitrile.

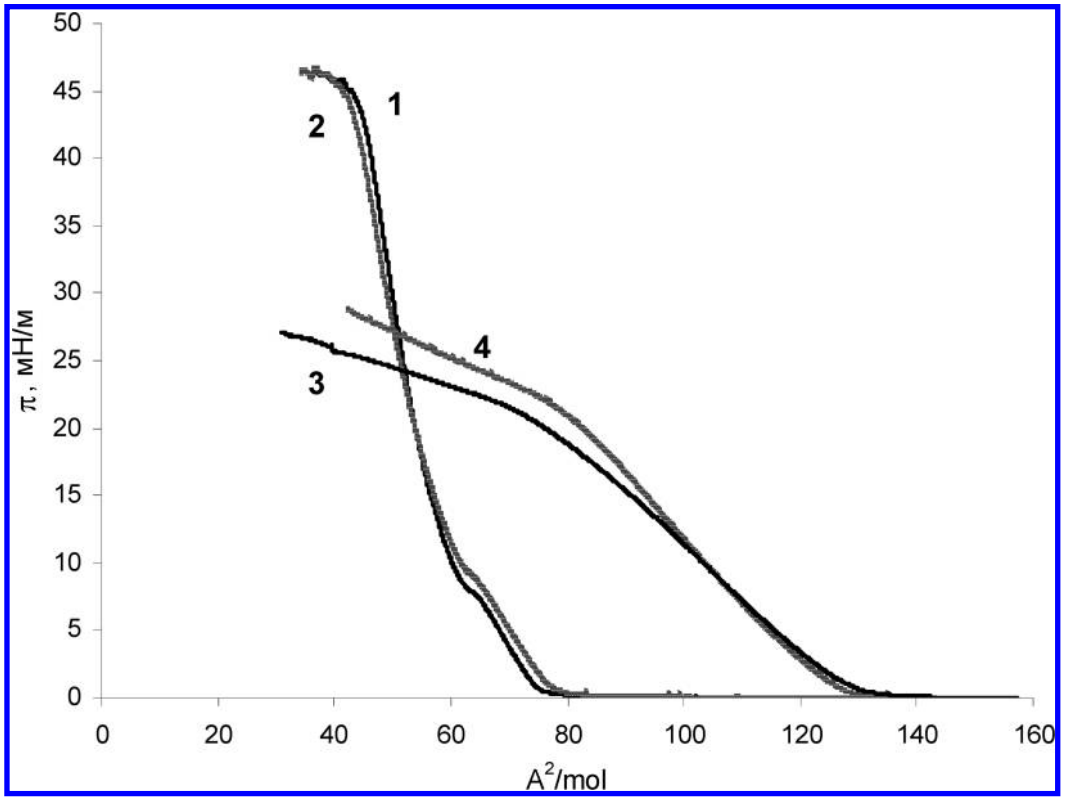

Figure 2. Surface pressure−molecular area isotherms of crown-substituted thiophene **I** (1−180 μL; 2−250 μL) and **II** (3−180 μL; 4−250 μL) monolayers at the air/water interface.

ether groups. We supposed that a combination of hydrophilic and lipophilic parts allows the formation of rather stable monolayers at the air/water interface. The hydrophobic oligothiophene parts of molecules would be disposed on the water surface, whereas lipophilic crown ether fragments are dipped into the water subphase.

Both molecules **I** and **II** contain a terthiophene moiety that is responsible for optical and electrochemical properties. In acetonitrile, solution compounds **I** and **II** exhibit strong absorption and fluorescence emission,[38,39,42,43] as shown in Figure 1.

Due to the linear structure, the styryl and terthiophene units in molecule **I** form an extended π-conjugated system. The resulting electronic absorption band is located in the visible region and centered at 450 nm (Figure 1(a)). The electronic absorption spectrum of the oligothiophene **II** is composed of two absorption bands (Figure 1(b)). The transition at high energy centered at ca. 330 nm could be attributed to the styryl chromophore, while the lowest energy band at 390 nm arises from the oligothiophene moiety. It was shown[43] that the terthiophene and styryl fragments in this molecule are optically independent. Thus, the difference between the positions of long-wavelength bands of the two compounds **I** and **II** is

dx.doi.org/10.1021/jp2074122 | J. Phys. Chem. B 2012, 116, 1482−1490

Scheme 2

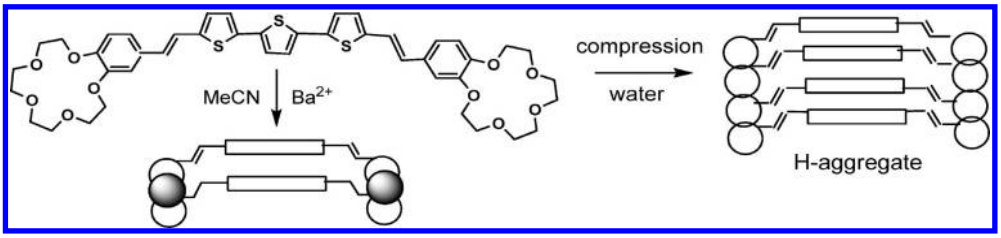

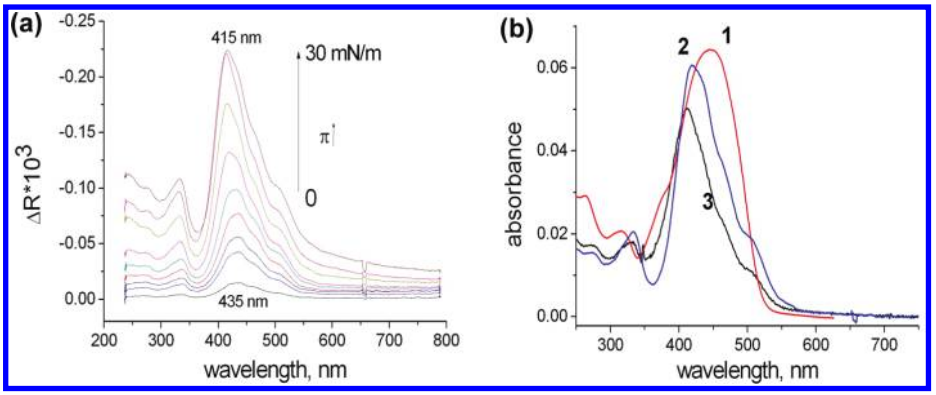

Figure 3. (a) Differential reflection spectra of **I** monolayer upon compression from 0 to 30 mN/m. (b) UV−vis spectra of **I** in acetonitrile (1) ([**I**] = 1.125×10^{-6} M), **I** monolayer at the air/water interface at 30 mN/m (2), and one-layer LB film of **I** on the quartz plate transferred at 30 mN/m (3).

directly linked to the different conjugation length of the chromophores.

According to the experimental data (Figure 2), crown-containing oligothiophenes **I** and **II** form stable monolayers on the water subphase. The surface pressure−molecular area isotherms (surface pressure (π)−area (A)) of both compounds remain unchanged upon varying the volume of spread solution from 180 to 250 μL (Figure 2).

The difference in geometry of the two isomers **I** and **II** greatly affects the shape and position of surface pressure−molecular area isotherms (Figure 2). Thus, the spreading ability of compound **I** is weaker than that of compound **II**. This leads to enhanced aggregation of molecules **I** in the monolayer via $\pi-\pi$ stacking of oligothiophene units at higher area per molecule. In addition, at low values of molecular area at which the surface pressure increases (80 Å^2/mol), the low compressibility of the monolayer and high pressure of collapse point out a perpendicular orientation of molecules of **I** on the water surface (Scheme 2, right).

In a previous study,[42] we found that the sandwich complex $[\mathbf{I}_2{\cdot}(Ba^{2+})_2]$ in which the two ligands **I** experience an H-aggregate association formed when barium perchlorate was added to an acetonitrile solution of **I** (Scheme 2). The sandwhich-like structure in which the metal cations are held between two crown ether units was favored because the ionic radius of Ba^{2+} (1.43 Å) is much larger than that of the crown ether moiety. A similar type of arrangement is also proposed for molecules **I** in the monolayer assembly. Moreover, it is well-known that oligothiophenes preferentially form an H-aggregate in the solid state.[44]

UV−vis spectroscopy allowed supporting this aggregate structure. Figure 3 shows the results of in situ measurements of the monolayer **I** at the air/water interface during the course of its compression. The differential reflection spectra (Figure 3(a)) of **I** clearly demonstrate that the lowest-energy absorption band (435 nm) of the compound **I** monolayer before compression is already hypsochromically shifted relative to the free compound in acetonitrile solution (450 nm), which shows that aggregation is effective at the air/water interface. Increasing the value of surface pressure up to 30 mN/m led to a blue shift of the spectrum, the band at 435 nm (spectrum at π = 0 mN/m in Figure 3) passing to 415 nm (upper spectrum in Figure 3(a)). Such a shift is usually attributed to the formation of H aggregates.[43,45−58] Thus, the H-aggregate formation of **I** starts upon spreading of the compound on the water surface and is completed by increasing pressure up to 30 mN/m. Interestingly, the release of surface pressure causes the recovery of spectral position of the long-wavelength band. This fact points to the reversibility of the aggregation process in monolayer **I**.

Monolayers of compounds **I** and **II** were vertically transferred onto quartz plates and the so-obtained one-layer (monolayer) LB films examined by UV−vis and fluorescence spectroscopy and compared to those recorded for the solution and monolayer at the air/water interface (30 mN/m).

The UV−vis spectra of oligothiophene **I** are presented in Figure 3(b). In both monolayers, aggregates of oligothiophenes **I** display a blue-shifted UV−vis spectrum with respect to the molecular solution. This indicates that the H-aggregate structure is preserved upon monolayer transfer onto quartz. It was found also that for LB films the intensities of all spectral bands increase upon increasing of the light incidence angle. This result testifies the vertical orientation of molecules in aggregates. The vertical arrangement of molecules in the monolayer implies the vertical orientation of the molecule plane relative to the subphase surface. Meanwhile, the axis of the oligothiophene chain is parallel to this surface in our case, and crown-substituted styryl fragments are arranged under the oligothiophene chain, as shown in Scheme 2.

In contrast, the results obtained with compound **II** point to a different behavior. Indeed, the in situ UV−vis measurements of compound **II** monolayers at the air/water interface demon-

dx.doi.org/10.1021/jp2074122 | J. Phys. Chem. B 2012, 116, 1482−1490

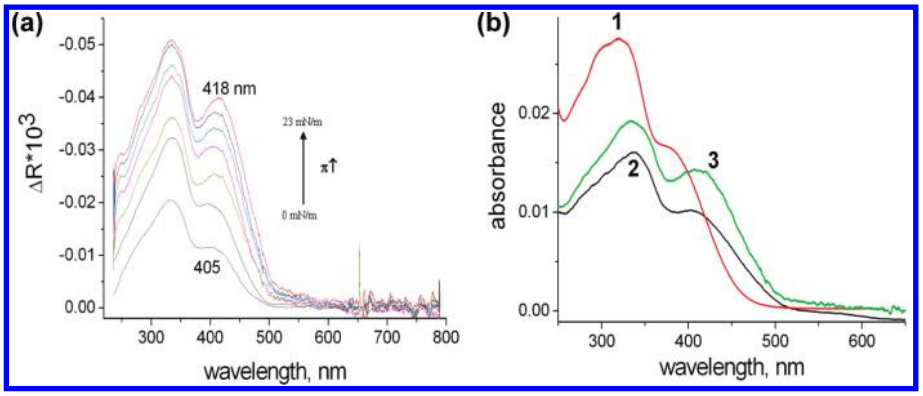

Figure 4. (a) Differential reflection spectra of monolayer **II** upon compression from 0 up to 23 mN/m. (b) UV−vis spectra of **II** in acetonitrile ([**II**] = 6.4×10^{-7} M) (1), monolayer **II** at the air/water interface at 23 mN/m (2), and one-layer LB film of **II** on the quartz plate transferred at 20 mN/m (3).

Scheme 3

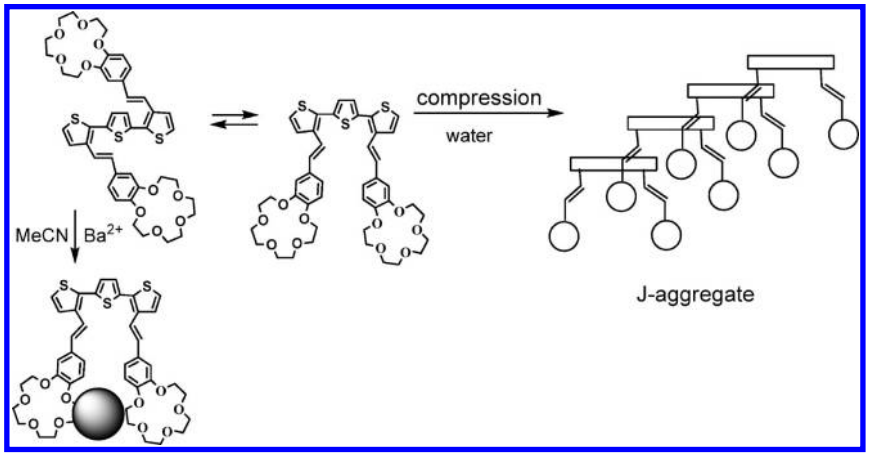

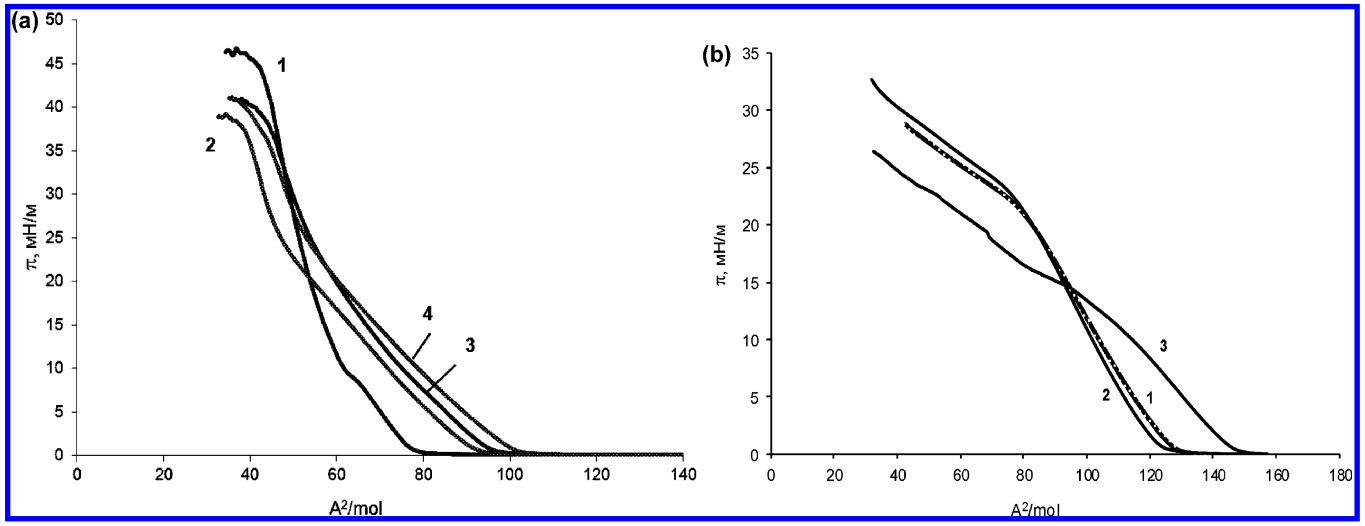

Figure 5. (a) Surface pressure−molecular area isotherms of monolayer **I** on distilled water (1) and subphase of different concentrations of $Ba(ClO_4)_2$ (2×10^{-5} M; 3×10^{-4} M; 4×10^{-3} M). (b) Surface pressure−molecular area isotherms of monolayer **II** on distilled water (1) and subphase of different concentration of $Ba(ClO_4)_2$ (2×10^{-4} M; 3×10^{-3} M).

strate that the low-energy absorption band, originating from the terthiophene unit, is bathochromically shifted relative to that obtained in acetonitrile and chloroform solutions (Figure 4). The two absorption bands of oligothiophene **II** in acetonitrile solution are located at ca. 330 and 390 nm (Figure 1(b)). The spectrum of monolayer **II** on the water surface before compression (π = 0 mN/m) displays two bands located at 330 and 405 nm (Figure 4). Upon monolayer compression from π = 0 mN/m to surface pressure value around 23 mN/m, the band at 405 nm is shifted bathochromically to 418 nm (Figure 4(a)). A pronounced bathochromic shift was also observed for **II** LB film (Figure 4(b)). It is observed that UV−

dx.doi.org/10.1021/jp2074122 | J. Phys. Chem. B 2012, 116, 1482−1490

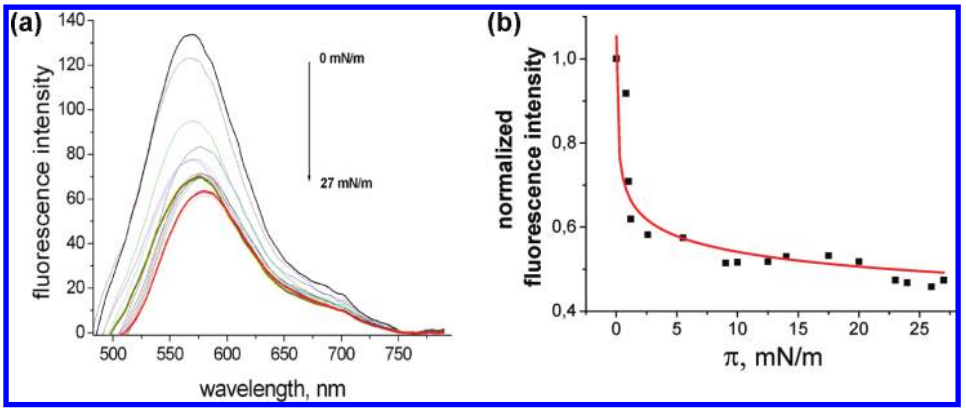

Figure 6. (a) Change of fluorescence spectra of monolayer **I** at the air/water interface upon monolayer compression. (b) Fluorescence intensity–surface pressure isotherm for monolayer **I** at the air/water interface.

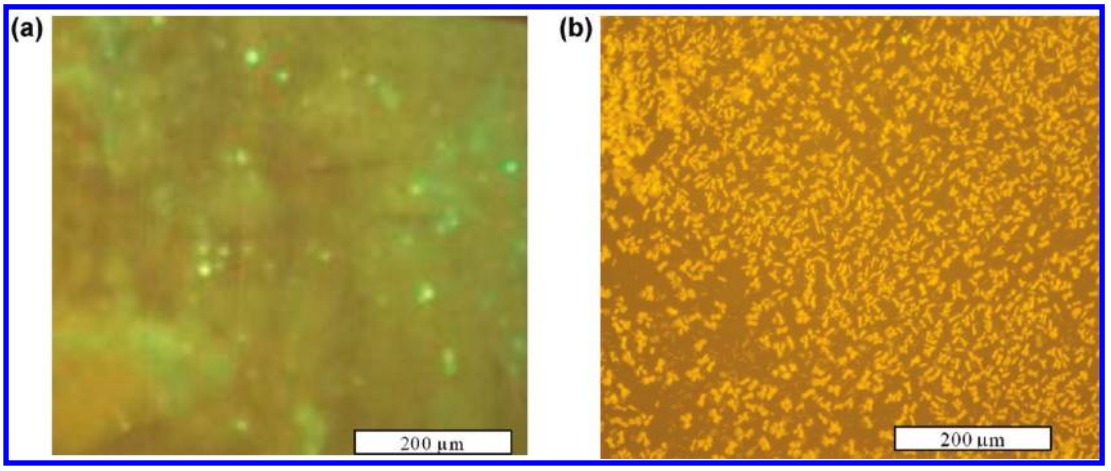

Figure 7. (a) Fluorescence microscopy image (BX51WI Olympus) of the one-layer LB film **I** transferred at 20 mN/m. (b) Fluorescence microscopy image (BX51WI Olympus) of the one-layer LB film **II** transferred at 20 mN/m.

vis spectra for the monolayer and the LB film of the compound **II** are similar (Figure 4(b)), indicating for this compound too that aggregate morphology is not altered upon transfer onto quartz.

To explain this behavior, it is necessary to consider that compound **II** is capable of changing the mutual arrangement of the two styryl fragments so that the molecule can have either a zigzag or a bent shape, leading to an *anti* or *syn* conformation, respectively. It has been shown that the latter conformation was observed[43] in complex [**II**·(Ba^{2+})] in acetonitrile (Scheme 3). This situation induced a bathochromic shift of the lowest-energy band in the UV–vis spectrum of the complex. It is reasonable to admit here that the *syn* conformation is the one that is likely to prevail at the air/water interface. Molecule **II** having such a conformation, the nonpolar thiophene units would be accommodated in the air phase, whereas hydrophilic crown-ether macrocycles would be dipped in the water subphase (Scheme 3). This situation can be explained in part by the bathochromic shift of the absorption, in connection with the case of the mononuclear barium complex. Also, with such a rearrangement of styryl fragments in **II** at the air/water interface, the *syn* conformers can adopt a staggered geometry in the aggregate at high surface pressure. In this case, the $\pi-\pi$ stacking interactions between thiophene units could possess a character of the J-aggregate, which could, in the ideal case, lead to a two-dimensional brickwork arrangement. It is indeed known that the formation of J-aggregates is accompanied by a bathochromic shift in absorption spectra.[45,49−52,56]

In the proposed structures of monolayers of both compounds, the crown ether moiety is located in the water phase and, thus, is able to interact with metal ions contained in the subphase. We prepared the monolayers on the $Ba(ClO_4)_2$ subphase and compare them with the monolayer on pure water (Figure 5(a),(b)). On the basis of the value of area obtained by extrapolation of the first linear part of the compression isotherm to $\pi = 0$, equal to 80 A^2/mol (Figure 5(a)), as well as spectral data for the monolayer (Figure 3(a)), we can conclude that both crown-ether groups of **I** are dipped into the subphase, whereas the plane of the hydrophobic thiophene part adopts a vertical orientation. An increase of surface pressure in this region is determined by contacts between polar groups of molecules. The second part of the curve with a lower compressibility shows the decrease of "free area" at compression of a rather compact monolayer. The presence of Ba^{2+} cations in the subphase results in expansion of monolayer due to electrostatic repulsion of these ions coordinated by crown-ether groups. This causes the lengthening of the isotherm first part due to the fact that the interaction between polar moieties becomes dominant. Thus, the observed effect confirms that the crown ether fragments are in the water phase.

The surface pressure–molecular area isotherm of monolayer **II** on distilled water starts from 130 A^2/mol which is larger than that for monolayer **I** (80 A^2/mol). The possible reason for the

dx.doi.org/10.1021/jp2074122 | J. Phys. Chem. B 2012, 116, 1482–1490

phenomenon could be that monolayer **II** compression is not accompanied by H-aggregate formation. Introduction of Ba^{2+} cations in the subphase in this case causes a monolayer expansion similar to that for the monolayer **I**.

Figures 5(a) and 5(b) show that in both cases the interaction between crown-substituted thiophenes and Ba^{2+} cations leads to the expansion of monolayers at the initial stage of compression. Such an effect may be connected with electrostatic repulsion between cations coordinated by the crown ether groups. Thus, the observed fact confirms that the crown ether fragments are in the water phase.

It was shown that addition of Ba^{2+} cations to the subphase did not affect practically the spectra of both systems. In both cases, monolayer spectra upon compressing on the barium perchlorate solution show the same shift of absorption bands as on the deionized water. This is explained by the weak complex formation between Ba^{2+} cations and oxygen crown ether in water solvent.

The in situ fluorescence measurements on monolayers of compound **I** at the air/water interface point to an increase in maximum emission red shift and fast decrease of normalized fluorescence intensity upon monolayer compression (Figure 6). Furthermore, monolayer **I** and LB film fluorescence spectra are red-shifted by more than 50 nm relative to the one of the solution.[42]

The morphology of the monolayer structures has been qualitatively characterized by fluorescence microscopy. The fluorescence microscopy image of **I** ultrathin film is shown in Figure 7(a). The film fluorescence emission is really weak. Some small fluorescent regions in the monolayer are visible in Figure 7(a), indicating the film heterogeneity, which can be associated with the presence of domains with nonaggregated oligothiophene **I**. The fluorescence quenching is in good agreement with literature data about the emission intensity decrease and the emission band shift to lower energies upon H-aggregation of oligomer chains and growth of aggregate length.[54,56−61]

Compound **II** LB film and monolayer fluorescence spectra are also red-shifted by about 50 nm relative to one of the solution. The fluorescence microscopy image shows that one-layer LB film produced from **II** molecules looks as a great number of strongly fluorescent needle domains composed from aggregated fluorescent *syn*-**II** molecules (Figure 7(b)).

The observation of fluorescence upon the monolayer **II** compression showed that an increase of the surface pressure from 0 to 16 mN/m causes the formation of a fluorescent structure (Figure 8). A subsequent increase in pressure is accompanied by a quenching of fluorescence emission. The profile of surface pressure−molecular area isotherm (Figure 2) also supports the proposition of two types of aggregation. It is believed that small (up to several molecules) aggregates formed in the low-pressure regime, under 0−16 mN/m, which serve as an "antenna" with high efficiency in fluorescence emission. A similar effect of fluorescence building-up for small associates of chromophore molecules possessing J-aggregate structure in Langmuir monolayers was described in ref 62. Further increase of pressure, beyond 16 mN/m, leads to two-dimensional aggregation in which intermolecular nonradiative deactivation pathways become efficient enough to quench fluorescence intensity.

Highly ordered structures made of ultrathin films provide advanced electronic properties. In addition, H-mode stacked conjugated chains are optimal for achieving high thin-film

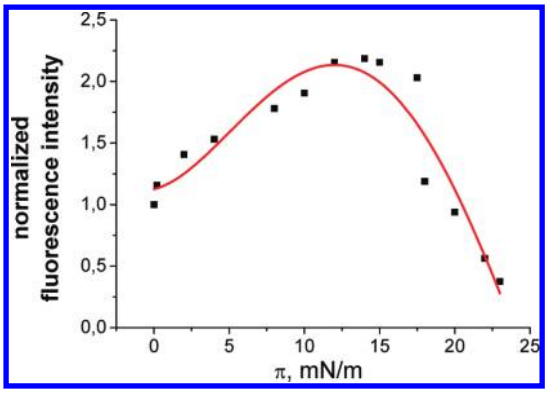

Figure 8. Fluorescence intensity−surface pressure isotherm for monolayer **II** at the air/water interface.

conductivity.[45,53,56,63] From this point of view, the investigation of electrochemical properties of oligothiophene LB films with different types of aggregates seems to be especially interesting and important. It should be noted that for molecule **I** in acetonitrile solution with Bu_4NClO_4 the cyclic voltammetric data showed the reversible oxidation process with values of potentials at forward and back traces, E_{pa1} = 0.70 V and E_{pc1} = 0.62 V, respectively, and $E_{(1/2)}$ = 0.66 V (Ag^+/AgCl). The oxidation process for **II** is irreversible because it is accompanied by electrodimerization on an electrode, E^{ox}_{pa}/E_{pc} = 0.96 V (Ag^+/AgCl).[38,42]

The thin films of compounds **I** and **II** were deposited onto gold-coated glass plates (SPR-electrodes) used as working electrodes in a three-electrode electrochemical cell. The cyclic voltammetric (CVA) measurements of the compound **I** LB films showed one-electron oxidation in the film (anodic peak at 0.56 V, cathodic peak at 0.50 V (Ag^+/AgCl)), and the electroactivity of the one-layer film is almost 100% (Figure 9).

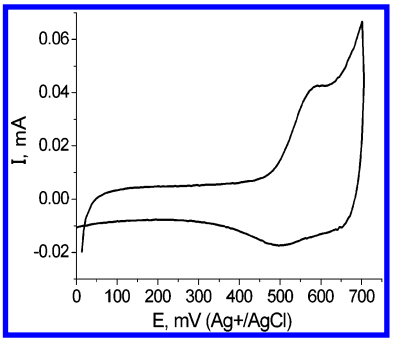

Figure 9. CV of compound **I** one-layer LB film (0.1 M $NaClO_4$, water, scan rate: 100 mV/s).

The relatively high value of the charging current in turn indicates the high conductivity of **I** LB film. In contrary, we failed to find red/ox peaks at CVA of **II** LB films. Such behavior can be connected with less conductivity of J-aggregated films as compared to the case of H-aggregated ones.[56,64]

The oligothiophene **I** LB film bistability based on red/ox switching was read using a surface plasmon resonance (SPR) technique. The stepwise change of electrode potential from 0.25 to 0.65 V and back is translated in an optical response, reflected in the stepwise change of resonance angle (Figure 10). These changes are reversible and registered in situ in a few seconds after the change of potential. This type of stepwise red/ox transformations of LB film can be useful for

dx.doi.org/10.1021/jp2074122 | J. Phys. Chem. B 2012, 116, 1482−1490

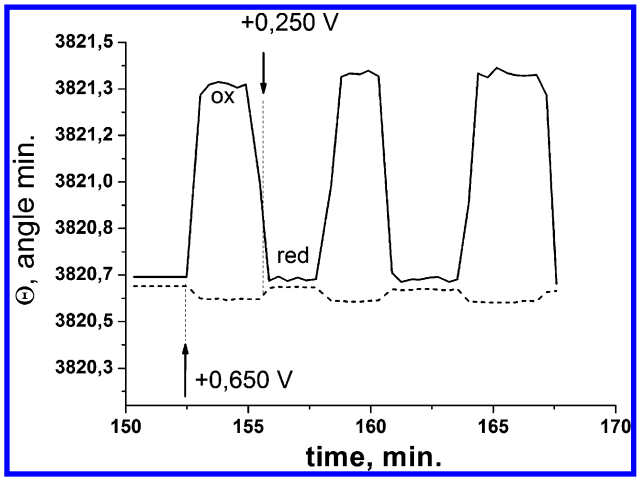

Figure 10. Changes of the resonance angle measured for the three-layer LB film of oligothiophene **I** (solid line) and for the bare gold support (dotted line) upon the stepped changes of electrode potential from 0.25 to 0.65 V and back.

development of switchable optoelectronic systems. The mechanism of optical response changes can be rather complicated. For example, the main parameter of the film which varies at red/ox transformations and influences the value of resonance angle in SPR measurements is the complex index of refraction. This coefficient in turn depends on the value of the molecular dipole in LB films, which are strongly connected with the molecule aggregate structure.

CONCLUSION

Two geometric isomers of oligothiophene derivatives containing two crowned styryl fragments in 2- or 3-positions of thiophene rings are able to form stable monolayers at the air/water interface. The difference in structure of oligothiophene molecules **I** and **II** leads to the formation of distinct monolayer architectures with differentiated electrochemical and optical characteristics.

For compound **I** bearing the styryl fragments at the 2-position of the terminal thiophene rings, the compression of monolayer leads to the formation of H-aggregates. Such types of aggregates in which the conjugated segments have an orientation perpendicular to the packing axis are responsible for quenching of monolayer fluorescence. A similar effect can also be observed in a one-layer LB film of **I** as well as the sandwich complex $[\mathbf{I}_2 \cdot (Ba^{2+})_2]$, having a H-dimer structure in solution. In addition, organization of oligothiophene **I** molecules in H-aggregates ensures the electrochemical activity of its LB films. Such a feature might be used for obtaining organic thin films with high conductivity and photovoltaic properties.

The styryl fragments in the compound **II** change their position from *anti-* in free ligand to *syn-* upon the monolayer formation at the air/water interface. The driving force in this case is the enhancement of amphiphilic characteristics of molecules, ensuring the possibility for hydrophilic crown ether fragments to interact with the aqueous subphase. In such a monolayer, the $\pi-\pi$ stacking interactions between thiophene units could possess a character of J-aggregate.

Monolayers of oligothiophenes of various structures can serve as models for the investigation of structure−property relationships in respect to finding the promising materials for organic electronics.

AUTHOR INFORMATION

Corresponding Author

*Phone: +7-4991358098. Fax: +7-4991350176. E-mail: fedorova@ineos.ac.ru.

ACKNOWLEDGMENTS

This work was supported by the programs of Ministry of Education and Sciences of Russian Federation and the Russian Foundation for Basic Research. In part this collaborative work was supported by GDRI CNRS 93 ≪Phenics≫.

REFERENCES

(1) Wurthner, F. *Angew. Chem., Int. Ed.* **2001**, *40*, 1037−1039.
(2) Katz, H. E.; Dodabalapur, V.; Torsi, L.; Elder, D. *Chem. Mater.* **1995**, *7*, 2238−2240.
(3) Fichou, D.; Dumarcher, V.; Nunzi, J.-M. *Opt. Mater.* **1999**, *12*, 255−259.
(4) Huisman, C. L.; Huijse,r, A.; Donker, H.; Schoonman, J.; Goossens, A. *Macromolecules* **2004**, *37*, 5557−5564.
(5) Lim, S.-T.; Shin, D.-M. *Synth. Met.* **2001**, *117*, 229−231.
(6) Era, M.; Yoneda, S.; Sano, T.; Noto, M. *Thin Solid Films* **2003**, *438*−*439*, 322−325.
(7) Loi, M. A.; Da Como, E.; Dinelli, F.; Murgia, M.; Zamboni, R.; Biscarini, F.; Muccini, M. *Nat. Mater.* **2005**, *4*, 81−85.
(8) Sullivan, J. T.; Harrison, K. E.; Mizzell, J. P.; Kilbey, S. M. *Langmuir* **2000**, *16*, 9797−9803.
(9) Singhal, R.; Chaubey, A.; Kaneto, K.; Takashima, W.; Malhotra, B. D. *Biotechnol. Bioeng.* **2004**, *85*, 277−282.
(10) Ochiai, K.; Rikukawa, M.; Sanui, K. *Chem. Commun.* **1999**, 867−868.
(11) Geiger, F.; Stoldt, M.; Schweizer, H.; Bauerle, P.; Umbach, E. *Adv. Mater.* **1993**, *5*, 922−925.
(12) Uchiyama, K.; Akimichi, H.; Hotta, S.; Noge, H.; Sakaki, H. *Synth. Met.* **1994**, *63*, 57−59.
(13) Marks, R. N.; Biscarini, F.; Zamboni, R.; Taliani, C. *Europhys. Lett.* **1995**, *32*, 523−528.
(14) Horowitz, G.; Delannoy, P.; Bouchriha, H.; et al. *Adv. Mater.* **1994**, *6*, 752−755.
(15) Shirota, Y. *J. Mater. Chem.* **2000**, *10*, 1−25.
(16) Mitschke, U.; Bauerle, P. *J. Mater. Chem.* **2000**, *10*, 1471−1507.
(17) Gamier, F.; Horowitz, G.; Peng, X.; Fichou, D. *Adv. Mater.* **1990**, *2*, 592−594.
(18) Gamier, F.; Hajlaoui, R.; Yassar, A.; Srivastava, P. *Science* **1994**, *265*, 1684−1686.
(19) Ostoja, P.; Guerri, S.; Rossini, S.; Servidori, M.; Taliani, C.; Zamboni, R. *Synth. Met.* **1993**, *54*, 447−452.
(20) Dodabalapur, A.; Torsi, L.; Katz, H. E. *Science* **1995**, *268*, 270−271.
(21) Simon, J.; Andrk, J.-J. *Molecular Semiconductors*; Springer-Verlag: Berlin, 1985.
(22) Muccini, M.; Mahrt, R. F.; Hennig, R.; et al. *Chem. Phys. Lett.* **1995**, *242*, 207−211.
(23) Adachi, C.; Tokito, S.; Tsutsui, T.; Saito, S. *Jpn. J. Appl. Phys.* **1988**, *27*, 269−271.
(24) Dodabalapur, A.; Rothberg, L. J.; Miller, T. M.; Kwock, E. W. *Appl. Phys. Lett.* **1994**, *64*, 2486−2488.
(25) Tessler, N.; Denton, G. J.; Friend, R. H. *Nature* **1996**, *382*, 695−697.
(26) Jousselme, B.; Blanchard, P.; Levillain, E.; Delaunay, J.; Allain, M.; Richomme, P.; Rondeau, D.; Gallego-Planas, N.; Roncali, J. *J. Am. Chem. Soc.* **2003**, *125*, 1363−1370.
(27) Otsubo, T.; Aso, Y.; Takimiya, K. *J. Mater. Chem.* **2002**, *12*, 2565−2575.
(28) Lopez-Cabarcos, E.; Retama, J. R.; Sholin, V.; Carter, S. A. Controlling the photoluminescence of water-soluble conjugated poly[2-(3-thienyl)ethyloxy-4-butylsulfonate)] for biosensor applications. *Polym. Int.* **2007**, *56*, 588−592.

(29) Yassar, A.; Gamier, F.; Deloffre, F.; Horowitz, G.; Ricard, L. *Adv. Mater.* **1994**, *6*, 660−663.
(30) Roncali, J. *Chem. Rev.* **1992**, *92*, 711−738.
(31) Demeter, D.; Blanchard, P.; Allain, M.; Grosu, I.; Roncali, J. *J. Org. Chem.* **2007**, *72*, 5285−5290.
(32) Burrell, K.; Chen, J.; Collis, G. E.; Grant, D. K.; Officer, D. L.; Too, C. O.; Wallace, G. G. *Synth. Met.* **2003**, *135/136*, 97−98.
(33) Si, P.; Chi, Q.; Li, Z.; Ulstrup, J.; Moller, P. J.; Mortensen, J. *J. Am. Chem. Soc.* **2007**, *129*, 3888−3896.
(34) Dinelli, F.; Murgia, M.; Levy, P.; Cavallini, M.; Biscarini, F. *Phys. Rev. Lett.* **2004**, *92*, 116802−1−116802−4.
(35) Murphy, A. R.; Chang, P. C.; VanDyke, P.; Liu, J.; Fréchet, J. M. J.; Subramanian, V.; DeLongchamp, D. M.; Sambasivan, S.; Fischer, D. A.; Lin, E. K. *Chem. Mater.* **2005**, *17*, 6033−6041.
(36) Marsella, M. J.; Swager, T. M. *J . Am. Chem. Soc.* **1993**, *115*, 12214−12215.
(37) Arslanov, V. V. *Russ. Chem. Rev.* **2000**, *69* (10), 883−898.
(38) Lukovskaya, E. V.; Bobyleva, A. A.; Fedorova, O. A.; Fedorov, Yu. V.; Anisimov, A. V.; Didane, Y.; Brisset, H.; Fages, F. *Russ. Chem. Bull.* **2007**, *56* (5), 967−974.
(39) Lukovskaya, E. V.; Bobyleva, A. A.; Fedorova, O. A.; Fedorov, Yu. V.; Anisimov, A. V.; Didane, Y.; Brisset, H.; Fages, F. *Russ. Chem. Bull.* **2009**, *58*, 1465−1470.
(40) Grüniger, H.; Möbius, D.; Meyer, H. *J. Chem. Phys.* **1983**, *79*, 3701−3710.
(41) Orrit, M.; Möbius, D.; Meyer, H.; Lehmann, U. *J. Chem. Phys.* **1986**, *85*, 4966−4979.
(42) Lukovskaya, E.; Bobylyova, A.; Fedorova, O.; Fedorov, Y.; Kardashev, S.; Maksimov, A.; Anisimov, A.; Maurel, F.; Marmois, E.; Jonusauskas, G.; Didane, Y.; Brisset, H.; Fages, F. *Synth. Met.* **2007**, *157*, 885−893.
(43) Lukovskaya, E.; Bobylyova, A.; Fedorov, Y.; Maksimov, A.; Anisimov, A.; Fedorova, O.; Jonusauskas, G.; Fages, F. *ChemPhysChem.* **2010**, *11*, 3152−3160.
(44) Videlot-Ackermann, C.; Ackermann, J.; Kawamura, K.; Yoshimoto, N.; Brisset, H.; Raynal, H.; El Kassmi, A.; Fages, F. *Org. Electron.* **2006**, *7*, 465−473.
(45) Reitzel, N.; Greve, D. R.; Kjaer, K.; Howes, P. B.; Jayaraman, M.; Savoy, S.; McCullough, R. D.; McDevitt, J. T.; Bjørnholm, Th. *J. Am. Chem. Soc.* **2000**, *122*, 5788−5800.
(46) Lednev, I. K.; Petty, M. C. *Langmuir* **l994**, *10*, 4185−4189.
(47) Lednev, I. K.; Petty, M. C. *J. Phys. Chem.* **1994**, *98*, 9601−9605.
(48) Wang, Y.; Ozaki, Y.; Iriyama, K. *Langmuir* **1995**, *11*, 705−707.
(49) Zhou, M.; Liu, H, L.; Yang, H. F.; Liu, X. L.; Zhang, Z. R.; Hu, Y. *Langmuir* **2006**, *22*, 10877−10879.
(50) Mobius, D. *Acc. Chem. Res.* **1981**, *14*, 63−68.
(51) Kuhn, H.; Mann, B.; Bucher, H.; Mobius, D.; Szentpaly, L. V.; Tillmann, P. *Photogr. Sci. Eng.* **1967**, *11*, 233−238.
(52) Kuhn, H. *Pure Appl. Chem.* **1979**, *51*, 341−352.
(53) Nakahara, H.; Fukuda, K.; Mobius, D.; Kuhn, H. *J . Phys. Chem.* **1986**, *90*, 6144−6148.
(54) Bjornholm, T.; Greve, D. R.; Reitzel, N.; Hassenkam, T.; Kjaer, K.; Howes, P. B.; Larsen, N. B.; Bogelund, J.; Jayaraman, M.; Ewbank, P. C.; McCullough, R. D. *J. Am. Chem. Soc.* **1998**, *120*, 7643−7644.
(55) Arslanov, V. V.; Gorbunova, Yu. G.; Selektor, S. L.; Sheinina, L. S.; Tselykh, O. G.; Enakieva, Yu. Yu.; Tsivadze, A. Yu. *Russ. Chem. Bull., Int. Ed.* **2004**, *53*, 2426−2436.
(56) McRae, E.; Kasha, M. *J. Chem. Phys.* **1958**, *28*, 721−722.
(57) Hoeben, F. J. M.; Jonkheijm, P.; Meijer, E. W.; Schenning, A P. H. J. *Chem. Rev.* **2005**, *105*, 1491−1546.
(58) Abraham, E.; Selector, S.; Grauby-Heywang, C.; Jonusauskas, G. *J. Photochem. Photobiol. B: Biol.* **2008**, *93*, 44−52.
(59) Lednev, I. K.; Petty, M. C. *Adv. Mater. Opt. Electron.* **1994**, *4*, 225−232.
(60) Xia, C.; Locklin, J.; Youk, J. H.; Fulghum, T.; Advincula, R. C. *Langmuir* **2002**, *18*, 955−957.
(61) Turshatov, A. A.; Bossi, M. L.; Möbius, D.; Hell, S. W.; Vedernikov, A. *Langmuir* **2006**, *22*, 1571−1579.
(62) Sergeeva, T. I.; et al. *Colloids Surf., A* **2005**, *264*, 207−214.
(63) Dimitrakopoulos, C. D.; Mascaro, D. J. *IBM J. Res. Dev.* **2001**, *45*, 11−27.
(64) Alfimov, M. V. *Herald Russ. Acad. Sci.* **2003**, *73* (No. 5), 429−439.